63 4

OFFICE OF NAVAL RESEARCH

Number 3511 (00)

Project Number 051 - 380

EXPERIMENTAL INVESTIGATIONS ON THE LIGHT SCATTERING OF COLLOIDAL SPHERES.
VI.   DETERMINATION OF SIZE DISTRIBUTION CURVES BY MEANS OF TURBIDITY
SPECTRA.

BY

MORTON L. WALLACH AND WILFRIED HELLER

TECHNICAL REPORT NO. 5 (51)

June 25, 1963

Submitted by

W. Heller, Project Director

Department of Chemistry

Wayne State University

Detroit, Michigan 48202

63 4

TO BE SUBMITTED FOR

PUBLICATION IN THE

JOURNAL OF PHYSICAL CHEMISTRY.

EXPERIMENTAL INVESTIGATIONS ON THE LIGHT SCATTERING OF COLLOIDAL SPHERES.
VI. DETERMINATION OF SIZE DISTRIBUTION CURVES BY MEANS OF TURBIDITY
SPECTRA.

By

Morton L. Wallach and Wilfried Heller

Department of Chemistry, Wayne State University, Detroit, Michigan

ABSTRACT

The usefulness of turbidity spectra for determining size
distribution curves is explored. The method is found to be equivalent
in performance to that based upon spectra of the scattering ratio
(depolarization) if the spectral turbidity maximum is within or near to
the spectral range investigated. Simultaneous investigation of turbidity
spectra and scattering ratio spectra provides a welcome check on the
distribution curve derived from either method.

EXPERIMENTAL INVESTIGATIONS ON THE LIGHT SCATTERING OF COLLOIDAL SPHERES. VI. DETERMINATION OF SIZE DISTRIBUTION CURVES BY MEANS OF TURBIDITY SPECTRA[1].

By

Morton L. Wallach[2] and Wilfried Heller

Department of Chemistry, Wayne State University, Detroit, Michigan

I. INTRODUCTION

The preceding paper in this series[3] dealt with a method for determining size distribution curves in heterodisperse systems of colloidal spheres by means of the spectra of the scattering ratio. An alternate method may be based upon the use of turbidity spectra. The theory of this alternate method has been given some time ago[4]. The present paper is concerned with the experimental test of this alternate method, using again heterodisperse polystyrene latices as model systems. The distribution curve is again assumed to be of the type

$$f(r) = (r-r_o)e^{-(r-r_o)/s)^3}$$

$$\text{and} \quad f(r) = 0 \text{ when } r < r_o \tag{1}$$

Here, $Cf(r)$ dr is the number of particles per unit volume of a system containing particles with radii between r and $r + dr$; r_o is the radius of the smallest particles present in consequential numbers[5] and s is a parameter proportional to the width of the distribution. For the definitions of the variousother quantities and parameters to be used, reference should be made to the preceding publications[3, 4].

---

1. This work was supported by the Office of Naval Research. The results given in the present paper were presented at the 134th meeting of the American Chemical Society, Chicago, September, 1958.

2. Present address: Film Department, E. I. DuPont & Co., Wilmington, Delaware.

3. W. Heller and M. L. Wallach, J. Phys. Chem. ..... .

4. M. L. Wallach, W. Heller, and A. F. Stevenson, J. Chem. Phys., 34, 1796 (1961).

5. Particles with a radius smaller than r_o are quantitatively defined here as those having a radius smaller than 99% of all the particles present in the system.

II. EXPERIMENTAL PROCEDURE

The systems investigated were the same as used previously[3].
They represent a positively skewed distribution (H.D. 1) in line with
eq. (1), a negatively skewed distribution (H.D. 2) and a Gaussian
distribution (H.D. 3). The apparatus used and preparation and treatment
of the latex samples were the same as in the preceding investigation[3].
Details of the optical set-up were the same as for turbidity measurements
on monodisperse systems[6] except for modifications already described[3],
introducing, in addition, the following changes: (1) On account of the
need for optimally monochromatic light, the radiation emerging from the
source was pre-monochromatized prior to its entry into the monochromator
proper by interposing interference filters combined with colored glass
filters; (2) The solid angle was decreased to 1.1×10^{-4} steradians in
order to eliminate, as much as possible, the contribution of forward
scattering[7].

Turbidity measurements were carried out at each wave length at
systematically varied concentrations, the lowest concentration within a
series being 0.24×10^{-5} ϕ, (ϕ: volume fraction of the polymer). The
specific turbidity, $\lambda \tau / \phi$, was then plotted against concentration and
extrapolated to infinite dilution. The spectra to be given pertain
therefore to the condition $\phi \to 0$, symbolized by $(\lambda \tau / \phi)_o$.

III. RESULTS

Figure 1 summarizes the specific turbidity spectra derived
from experiment for the three systems[8]. The shapes of the curves differ

---

6. R. M. Tabibian, W. Heller, and J. N. Epel, J. Coll. Sci., 11, 195 (1956).

7. For a discussion of this effect see R. M. Tabibian and W. Heller, J. Colloid Sci., 12, 25 (1957).

8. The width of the rectangles represents the maximum uncertainty in λ_o; their height is the maximum uncertainty in $(\tau / \phi)_o$. The data indicated by the black dots are the most probable values. In the case of H.D. 3, the combined use of an Hg vapor lamp (instead of the Pointolite lamp used in the other two cases) a monochromator, and interference filters, reduced the former uncertainty to a graphically negligible value at two of the three wave lengths used.

characteristically. The turbidity maximum is seen to move towards shorter wavelengths in the direction $- H.D.2 \rightarrow H.D.1 \rightarrow H.D.3$. This indicates, as will be seen, a decrease, in this direction, of the modal diameter, D_m. The direction in the shift is therefore qualitatively the same as that expected in monodisperse systems.

In order to derive distribution curves, the experimental spectra are compared with a series of theoretical spectra constructed by using suitable pairs of p_R and q_R-values. For this purpose, it is advantageous to normalize both types of spectra with respect to the specific turbidity observed at a reference wavelength. The reference selected here is the green Hg-line. This normalization eliminates (a) uncertainties connected with concentration determinations and (b) corrections in the numerical values associated with the finiteness of the solid angle[7] and (c) it allows one to accomodate several spectra in a single graph.

The normalized experimental $\lambda \tau/\phi$-spectra are represented in Figs. 2 and 3 by the heavily drawn curves. The open circles correspond to the most probable experimental values given in Fig. 1. The black circles are obtained by interpolation by means of the curves in Fig. 1. Normalized theoretical spectra are derived by first varying the values of q_R-p_R pairs within large intervals. Having come reasonably close to the normalized experimental spectra, the intervals in the numerical values of q_R and p_R are reduced to 0.4 or 0.2. (After some experience, the first step of wide variations in q_R and p_R can be eliminated). Three (Fig. 3) or four (Fig. 2) theoretical spectra are reproduced for each of the three systems. They cover the entire range of acceptable q_R-p_R combinations which form the basis for the subsequent selection of the best q_R-p_R-pair. This final selection may be made by simply picking that theoretical spectrum which comes closest to the experimental one. Instead, one may, for a still better approximation, obtain the optimal q_R-p_R-pair by interpolation between the two or three closest fitting theoretical spectra. The spectra used for such interpolations are identified in

Figs. 2 and 3 by the symbols i_1 and i_2 respectively[9].

Figures 4, 5, and 6 give the optical distribution curves and electron microscopic histograms obtained for H.D. 1, H.D. 2, and H.D. 3, respectively. (The procedure used for the electron microscopic determinations of the size distributions has been described previously[3].) The fully drawn curve in Fig. 4 (H.D. 1) results from the interpolated q_R and p_R-values intermediate between those of the i_1 and i_2 spectra in Fig. 2[10]. The dotted curves pertain to the i_1 and i_2 spectra themselves. The modal diameter is hardly affected by the interpolation. On the other hand, the peak height of the curve is improved by it. Figure 5 (H.D. 2) contains only the curve obtained by interpolation between the i_1, i_2, and i_3 curves (see Fig. 3 and Footnote 9). Fig. 6 gives two distribution curves (I, II) derived for H.D. 3 from the i_1 and i_2 pairs of q_R-p_R-values (see Fig. 2). The distribution curve which would result from an interpolation between the i_1 and i_2-pairs is omitted. It would be intermediate between the curves I and II.

The method applied here for the derivation of size distribution curves from turbidity spectra is based on the spectra obtained by extrapolation of ($\lambda \tau / \phi$)-values to zero concentration at all wavelengths. This is time consuming. It is therefore of interest to note that it may be sufficient to operate at a single reasonably small concentration if optimum accuracy is not required for the distribution data. Although the individual $\frac{\lambda \tau}{\phi}$ -values are then different from the extrapolated ($\lambda \tau / \phi$)-values, the shape of the normalized $\frac{\lambda \tau}{\phi}$ vs. λ_o curve is not materially affected. This is tested for H.D. 1. Normalized data of $\lambda \tau / \phi$ obtained at the very small concentration of 0.827×10^{-3} g. solids/100 g. latex are identified by crosses in Fig. 2.

---

9. In order not to crowd Figs. 2 and 3, only 3 or 4 instead of the larger number of actually considered theoretical spectra are shown. For the same reason, the i_2-curve in Fig. 2, pertinent to H.D.3, is omitted (q_R:1.8; p_R:5.6). Similarly, an i_3-curve in Fig. 3 (1.8; 7.2) is omitted.

10. Electronic computation would, of course, carry out automatically the equivalent of such interpolations.

They are throughout larger than those obtained by extrapolation of
the spectrum to zero concentration (circles). The q_R-p_R pair satisfy-
ing these alternate data (1.0; 7.0) would give a distribution curve
very similar to that of the pair (1.0; 7.2) except for a slightly lower
modal diameter. On using this approximation method, it is really not
necessary to know the absolute concentration provided that one has
proof that one operates within "safe" range of low concentrations. The
safe range is defined by the fact that τ varies, within it, linearly
with concentration at all wavelengths used (negligible multiple
scattering).

Table I gives a comprehensive survey of the numerical results
obtained for the number average diameter, $\bar{D}_n$, modal diameter, D_m, dia-
meter of the smallest particle present in consequential numbers, D_o,
and the halfwidth, W^{11}. In each instance, the per cent deviation with
respect to the electron microscopic data is given in parenthesis. The
quantities enumerated being those of principal importance, it can be
stated that the method employed here for determining size distribution
curves is most satisfactory in those cases where the basic type of uni-
modal distribution curve does not differ from that assumed. If the
distribution curve is not of the type assumed, the results for $\bar{D}_n$, D_m
and D_o are still very satisfactory, but the halfwidth W is obviously
very much in error. If better results for the latter are to be ob-
tained, it is necessary to use the two term equation or equivalent
procedures discussed previously[3]. It is, fortunately, easy to ascertain
when this contingency arises. A major departure of the distribution
curve from that assumed by eq. (1) is indicated by the fact that no
theoretical spectrum can be found—by means of any q_R-p_R-combinations—
which would coincide with the experimental spectrum except for a very
narrow spectral range. In Fig. 2 the experimental spectral curve of

---

11. The halfwidth W considered here is twice the halfwidth, w, de-
fined previously[2]. The latter would apply if the independent
variable were the particle radius, r, rather than the diameter
used here.

H.D. 1-which satisfies eq. (1) is nearly parallel to any of the best
fitting theoretical curves. On the other hand, in Fig. 3, any theoretical
curve which is fitting well in one part of the spectral range considered,
crosses the experimental curve in another part. This indicates at once
that the system investigated does not possess the distribution assumed.
For the Gaussian distribution in Fig. 2 (H.D. 3) the situation is inter-
mediate. Here, it is seen from the degree of agreement between experi-
mental and theoretical spectra that the distribution curve differs, but
not radically, from that assumed. It depends of course on the objective
as to whether or not unsatisfactory compliance of the best theoretical
and the experimental spectrum warrants use of the more time consuming
two term equation or of its equivalents. The "worst case" that one may
face with unimodal distributions, is that illustrated by Fig. 5. For
many purposes, such an approximate distribution curve may be sufficient.

IV. APPROXIMATION METHODS AND METHODS FOR ATTAINING LIMITED OBJECTIVES.

Approximating procedures are indicated if the objective is
merely the determination of $\bar{D}_n$, D_m, and D_o. The reason is that D_m and
$\bar{D}_n$ change relatively little on varying q_R and p_R within modest limits.
This is clear from the pertinent equations given previously[12]. There-
fore the agreement between the electron microscopic modal diameter and
that derived from any of the curves in Figs. 2 and 3 is within 7%, 3%,
and 2% for H.D. 1, H.D. 3, and H.D. 2 respectively. If the objective
is therefore limited to any or all of these three data, it is not
necessary to search for the best fitting theoretical spectrum. An ap-
proximate fit is then all that is needed.

If the objective is even more limited, i.e., if one is merely
interested in determining an approximate value of D_m or $\bar{D}_n$, one may
dispense with spectra entirely and operate at a single wavelength. The
diameter thus obtained is an apparent quantity since the system is
treated as if it were monodisperse. It is of interest to evaluate

12. A. F. Stevenson, W. Heller, and M. L. Wallach, J. Chem. Physics,
34, 1789 (1961).

the error committed by using such a very simple technique on hetero-
disperse systems. Choosing, for this purpose, the data obtained at
the green mercury line, the theoretical specific turbidities would
yield a particle diameter of 1.196 , 1.214 , and 0.736 μ for H.D. 1,
H.D. 2, and H.D. 3, respectively. The differences between these dia-
meters and modal diameters as obtained from the optical distribution
curves are 15, 10, and 21% respectively. The numerical error would be
larger than indicated in systems more heterodisperse than those used
here and smaller in the reverse case. Similarly, in a given system, the
error would obviously vary with the wave length. Therefore, the ratio
of the apparent diameters obtained at two wavelengths-treating the
system as if it were monodisperse (q = 0)-can provide a rough measure
of the relative degree of heterodispersion[13]. Only in strictly mono-
disperse systems can this ratio be equal to 1.0 provided the difference
in the refractive index at the two wave lengths used is taken into account.

V. PROBABLE RANGE OF USEFULNESS OF TURBIDITY SPECTRA.

The usefulness of turbidity spectra (within the visible spectral
range) for determining size distribution curves and the sensitivity of
the spectra to changes in the degree of heterodispersity have been in-
vestigated in the present work for size distribution curves extending
from particle diameters of about 0.7 to 1.4 microns. It can be anti-
cipated that a sensitivity of $(\lambda c/\rho)_o$-spectra to heterodispersion,
similar to that found here, exists also for particles smaller than 0.7
microns (but large enough to be outside of the range of Rayleigh
scattering)[14]. While experiments in this lower range are desirable, the

---

13. It is clear that the apparent diameter should increase with de-
creasing wavelength if the spectral range considered comprises
wavelengths larger than that at which the spectral maximum occurs.
It should decrease with decreasing wavelength in the inverse case.

14. The method described here like any other possible light scattering
method will, of course, be wholly insensitive to particle size
distributions if all the particles are so small compared to the
wavelength that Rayleigh scattering applies.

situation which one is bound to find if D_o is as small as 0.26 micron (p_R = 2.0) can be derived from an inspection of Fig. 3 of reference 4. An increase of q_R from 1.0 to 4.0 leads to about the same change in the normalized $(\lambda \tau/\phi)_o$-spectrum if p_R has the constant value of 6.0 ($D_o \sim 0.8 \mu$) in one case and 2.0 in another.

On the other hand, turbidity spectra will fail if the particles are too large relative to the wave length. Work done by R. Wu in continuation of the present work shows that the sensitivity of the turbidity spectra method within the visible range of the spectrum begins to fall off seriously if the distribution extends to diameters as large as two microns.

On being faced with systems in which the particles are too small (Rayleigh range) or too large (upper microscopic range) to apply usefully turbidity spectra within the visible range, one may, of course, in favorable instances (no or weak true absorption), resolve the problem by making use of turbidity spectra in the far ultraviolet or intermediate infrared respectively.

VI. COMPARISON OF THE PRESENT METHOD WITH THAT BASED ON THE SPECTRA OF THE SCATTERING RATIO.

The results presented here, on comparing them with those given previously[3], show that the method of determining size distribution curves from turbidity spectra is, at least for the systems investigated, comparable in performance to that based upon spectra of the scattering ratio. A specific example is given in Fig. 6. The size distribution curve obtained for H.D. 3 from σ-spectra (Curve III) is compared to those obtained by the method described in this present paper. The curves are in satisfactory agreement. For a closer check, the results given in Table I may be compared with the results obtained for the same systems by the alternate method (see Table I, Ref. 3). An important advantage of the present method is its relative simplicity inasmuch as any properly modified spectrophotometer may be used. In addition, due to their monotonic character, theoretical $(\lambda \tau/\phi)$ (λ)-curves can be

derived and constructed factor[15]. Also, a high brightness of the light source is not as imperative here as in the case of scattering ratio spectra.

On the other hand, an advantage of the method based upon spectra of the scattering ratio is that the curves are more oscillatory and should, therefore, in principle, be more sensitive to changes in heterodispersity. They should also be relatively independent of p_R (the smallest particle size at which the distribution curve effectively begins) except for the inconvenience of having a large number of maxima and minima within a limited spectral range if one were to operate within the microscopic range. This may well be the most important advantage over the turbidity spectra which should, as stated, become rather insensitive to size distributions if D_o is in the microscopic range.

An important further difference between the method of σ-spectra and turbidity spectra pertains to the ease of finding the q_R and p_R-values to be used for the analysis. This is of major practical importance if the fitting of theoretical and experimental spectra is not carried out by electronic computation. In order to lose as little time as possible in picking the right range of q_R-and p_R-combinations out of an a priori infinite number of combinations, one uses as a guide the general aspect of the experimental spectra. There are two arguments in the case of the σ-spectra. The number of maxima and minima within a given spectral range gives the range of p_R-values to be examined. Their degree of shallowness gives the range of q_R-values to be examined, (see e. g. figs. 4, 5, 6 in ref. 12). In the case of the turbidity spectra, on the other hand, the number of possible maxima is reduced to one. A quick analysis is therefore possible only if the $\lambda \tau / \phi$ maximum occurs within the visible range. The presence of such a maximum immediately limits the number of p_R-values that may be considered. The degree of shallowness of the maximum is a reliable indicator of the approximate q_R-range to be considered. The two arguments are therefore, under these circumstances,

---

15. This advantage is, of course, minor if electronic matching is used.

similar to those enumerated for the σ-spectra. The absence of a
maximum within or very close to the experimental spectrum of $(\lambda c/\phi)$
increases the labor of finding the best q_R-p_R-pair; it does, however,
not interfere with the applicability of the $\lambda c/\phi$-method. Only one of
the three systems investigated here, exhibited a $\lambda c/\phi$ maximum.

The availability of both the $\sigma(\lambda)$ and $\lambda c/\phi(\lambda)$ methods provides
a welcome opportunity to check the results obtained with one against
those obtained with the other. It allows one to make a quicker decision
as to the proper q_R and p_R-combination than with one spectrum alone.
Furthermore, a combination of the two methods, and, if necessary, consid-
eration of a third (variation of lateral scattering with the angle of
observation)-may allow one to derive distribution curves without having
to make any assumption about its basic type. This possibility which
appears very promising, provided the degree of heterodispersion is not
so large as to wipe out spectral and angular maxima and minima completely,
is being explored at the present time.

In conclusion, it may be noted, that with systems in which the
spheres show a strong dispersion (of the refractive index) dispersion
corrections may be indicated on applying the method described here.
With the systems investigated here, these corrections proved to be too
small to be taken into account.

TABLE I

Summary of Numerical Results.

All data are in microns except bracketted data which represent per cent deviations relative to electron microscopic data.

System	$\overline{D}_n$	D_m	D_o	W
H.D. 1	1.02_8 (6.5)	1.02_0 (5.6)	0.91_2 (3.3)	0.14_1 (~1)
H.D. 2	1.10_2 (3.3)	1.09_3 (0.6)	0.95_5 (4.5)	0.18_0 (26)
H.D. 3	0.90_0 (2.5)	0.88_8 (2.1)	0.71_7 (6.5)	0.22_3 (27)

Figure 1. Actual (r/ϕ)-spectra of the heterodisperse systems H.D. 1 and 3 investigated.

Numerical data identifying the three characteristic parameters of the distribution curves are due to electron microscopy (subscript e). Dots: most probable values; height of rectangles: total width of spectral band entering apparatus. (In two instances, use of Hg-vapor lamp, instead of incandescent source-in combination with monochromator, interference filters and color filters-reduced width of rectangle to practically zero.)

Figure 2. Normalized experimental and theoretical $(\lambda r/\phi)_0$-spectra of H.D. 1 and H.D. 3.

Heavily drawn curves: Spectra derived from experiment.
Other curves: theoretical spectra.

Figure 3. Normalized experimental and theoretical $(\lambda r/\phi)_0$-spectra of H.D. 2.

Figure 4. Size distribution curves derived from turbidity spectra and comparison with electronmicroscopic histogram. I: System (H.D. 1) with positively skewed distribution conforming to eq. (1).

Fully drawn curve: using interpolated q_R-p_R-values.
Dotted curves: using the two q_R-p_R-pairs which come closest to achieving spectral fit on using Δq_R and Δp_R intervals of 0.4.

Figure 5. Size distribution curve derived from turbidity spectra and comparison with electronmicroscopic histogram. II: System (H.D. 2) with negatively skewed distribution curve.
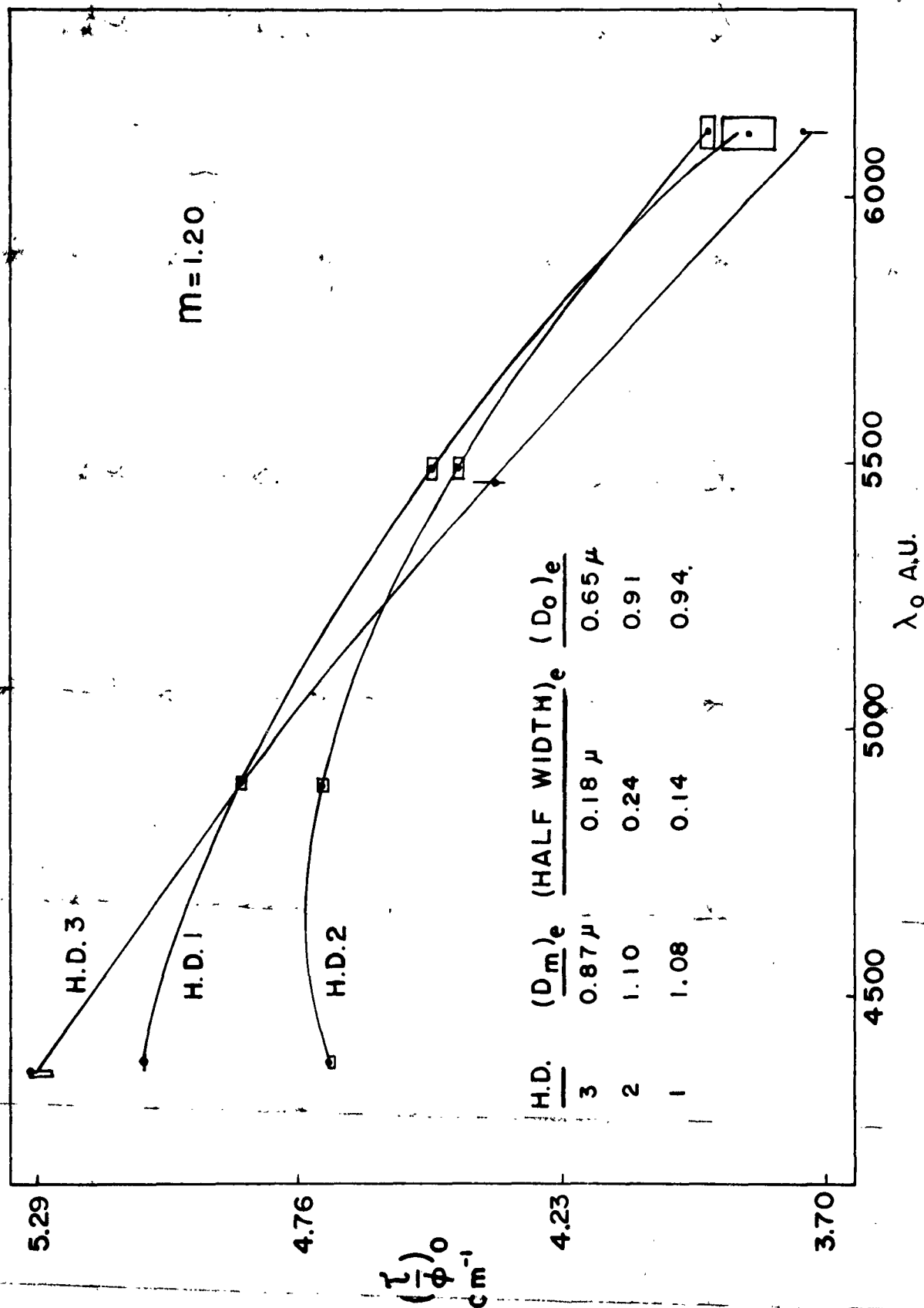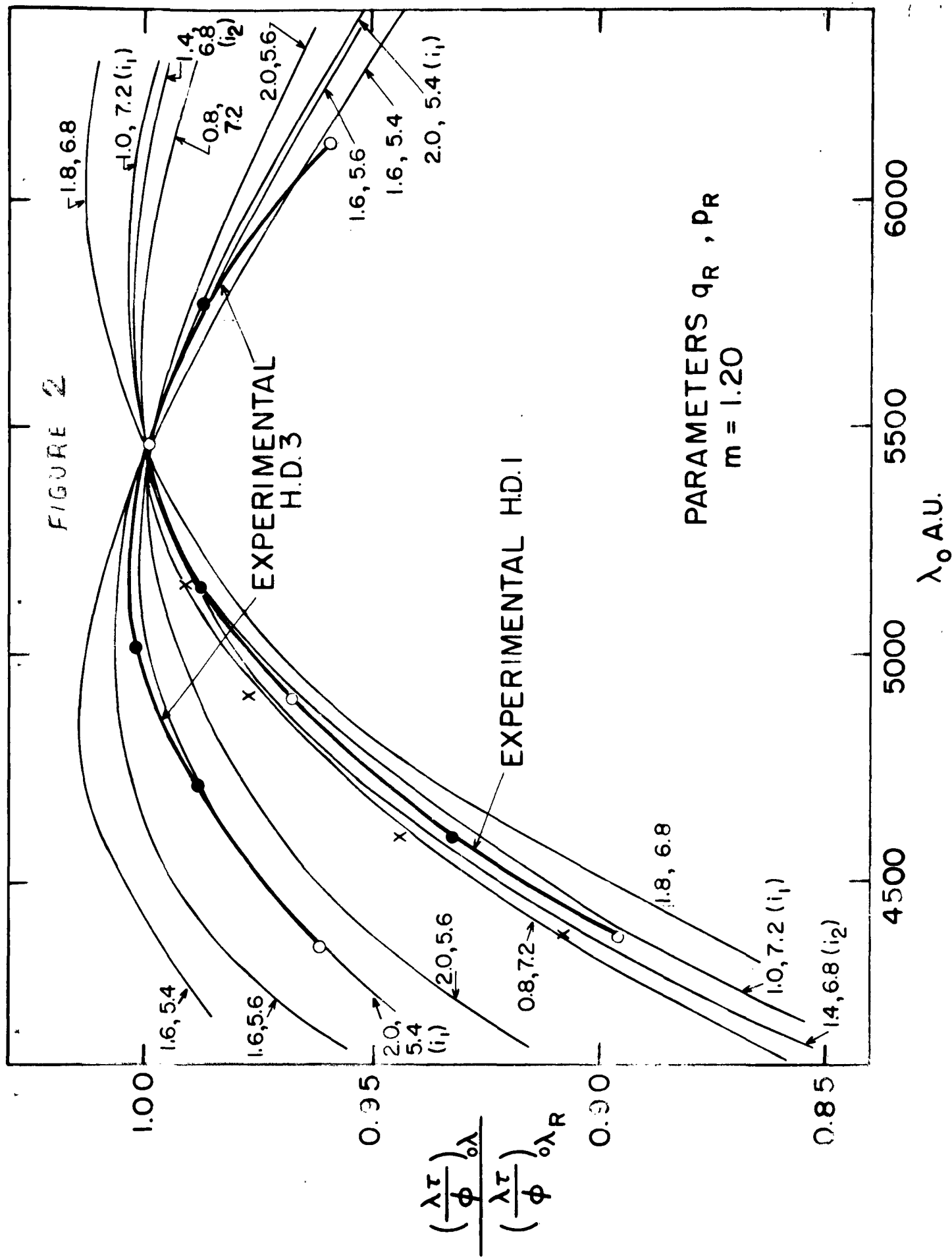
Interpolated q_R-p_R-values used.

Figure 6. Size distribution curves derived from turbidity spectra and comparison with curves obtained from spectra of scattering ratio and with electronmicroscopic histogram. System (H.D. 3) approximating Gaussian distribution.

I, II: using turbidity spectra and the two q_R-p_R pairs which came closest to achieving spectral fit on using Δq_R-and Δp_R-intervals of 0.2. (Interpolation of q_R and p_R-values would yield curve within area bounded by curves I and II.)
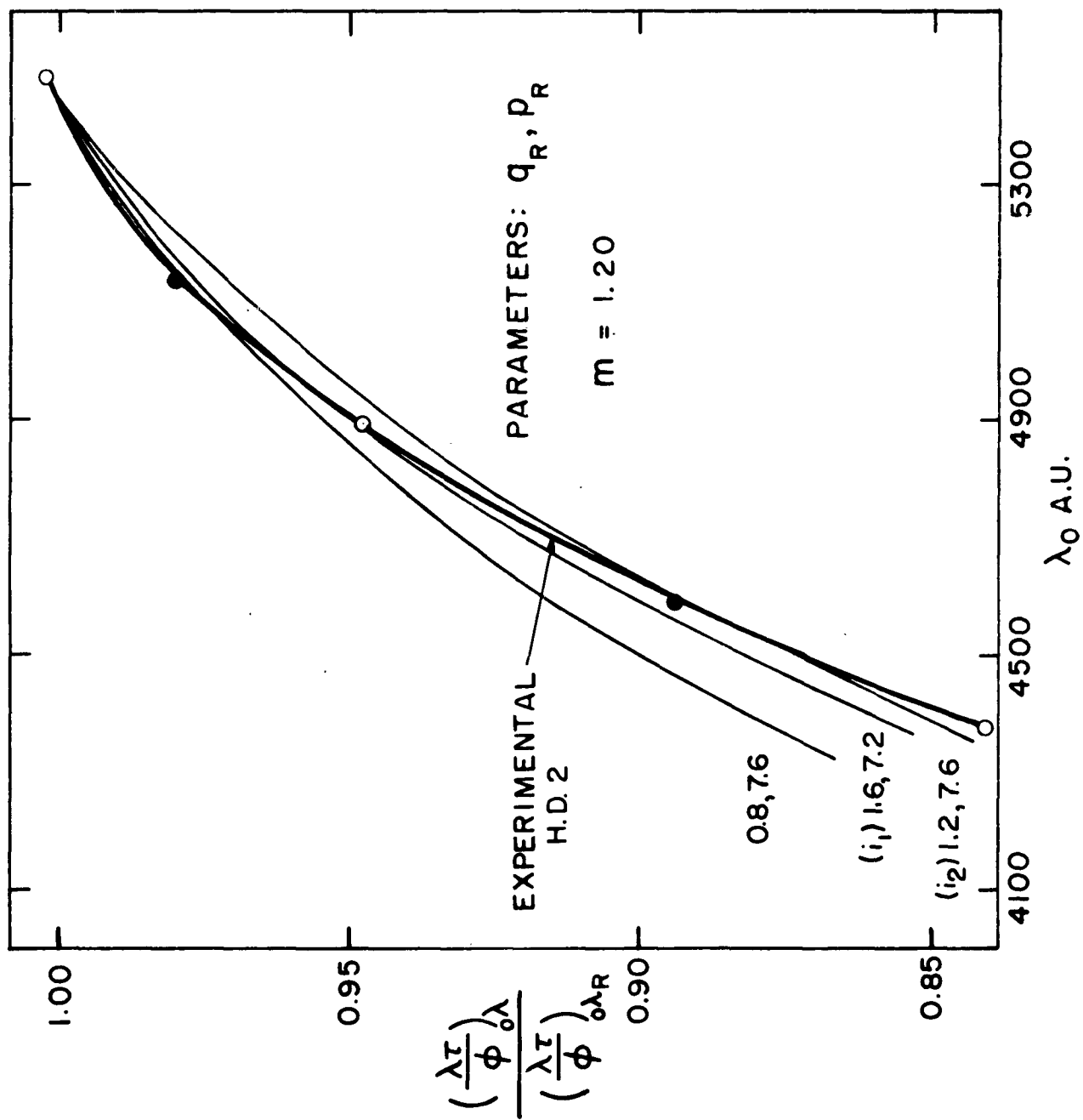
III: using σ-spectra and interpolated q_R-and p_R-values.

TR 51
FIGURE 1
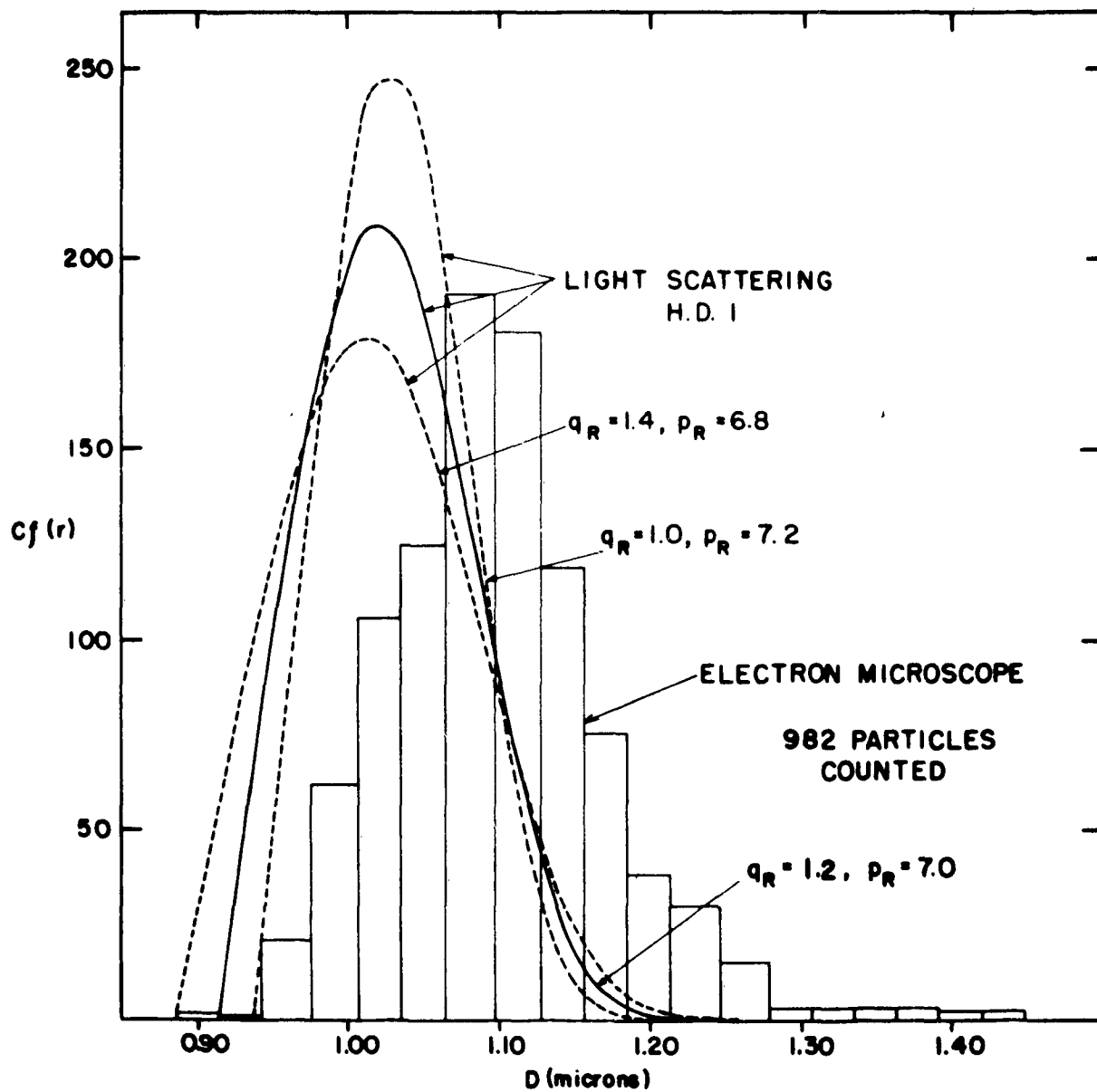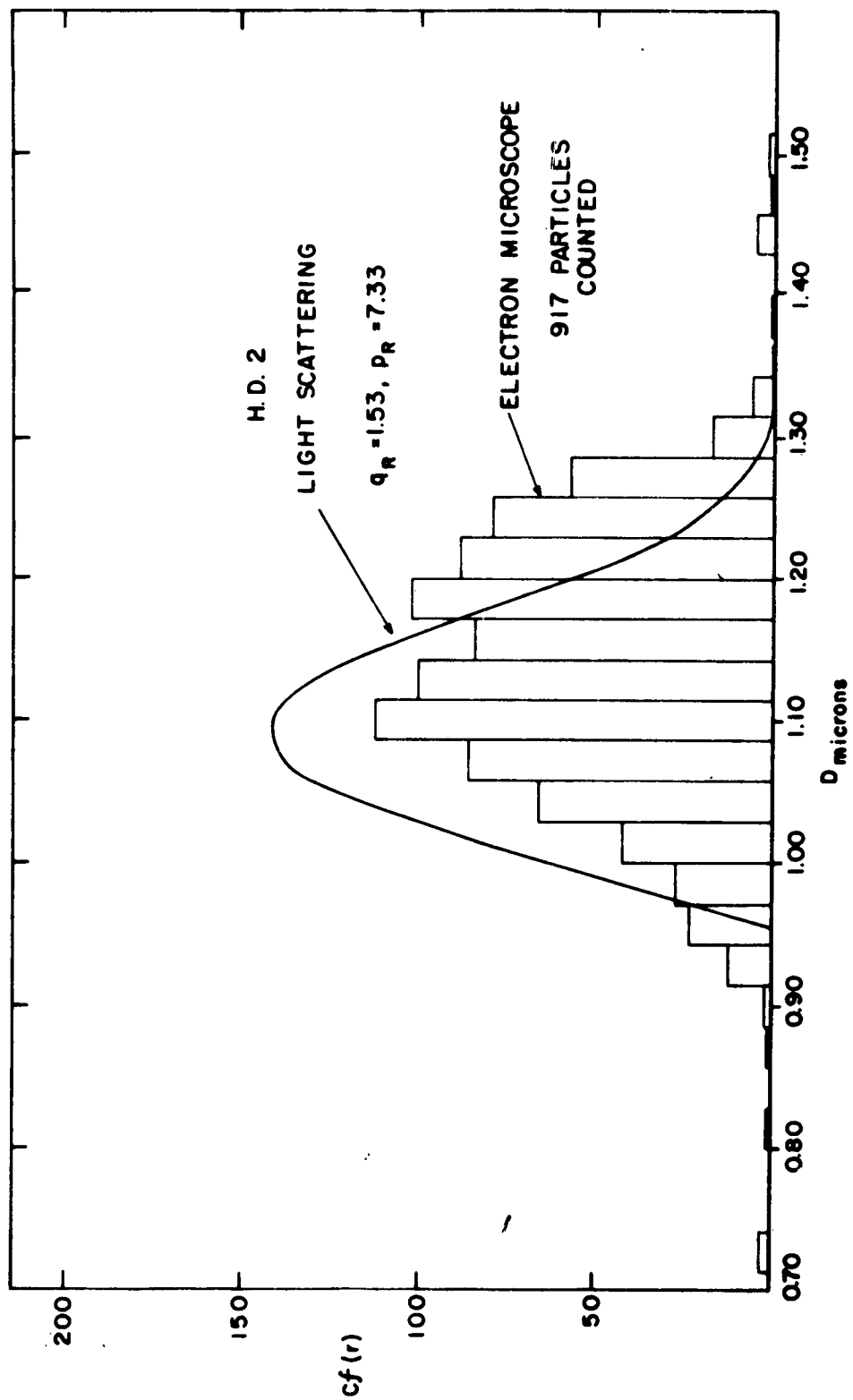
FIGURE 2

PARAMETERS q_R, p_R
m = 1.20

FIGURE 3

LIGHT SCATTERING
H.D. I

q_R =1.4, p_R =6.8

q_R =1.0, p_R =7.2

ELECTRON MICROSCOPE

982 PARTICLES
COUNTED

q_R = 1.2, p_R = 7.0

$Cf(r)$

D (microns)

H.D. 2

LIGHT SCATTERING

$q_R = 1.53$, $p_R = 7.33$

ELECTRON MICROSCOPE

917 PARTICLES COUNTED

$D_{microns}$

$cf(r)$

200

150

100

50

0.70   0.80   0.90   1.00   1.10   1.20   1.30   1.40   1.50

FIGURE 6

FR-51

H.D. 3

LIGHT SCATTERING

$q_R = 2.0$, $p_R = 5.4$

$q_R = 1.8$, $p_R = 5.6$

FROM TURBIDITY SPECTRA

ELECTRON MICROSCOPE

1192 PARTICLES COUNTED

FROM SCATTERING RATIO SPECTRA
$q_R = 1.90$, $p_R = 5.65$

$cf(r)$

200

150

100

50

0.60   0.70   0.80   0.90   1.00   1.10   1.20   1.30   1.40

D (micron)
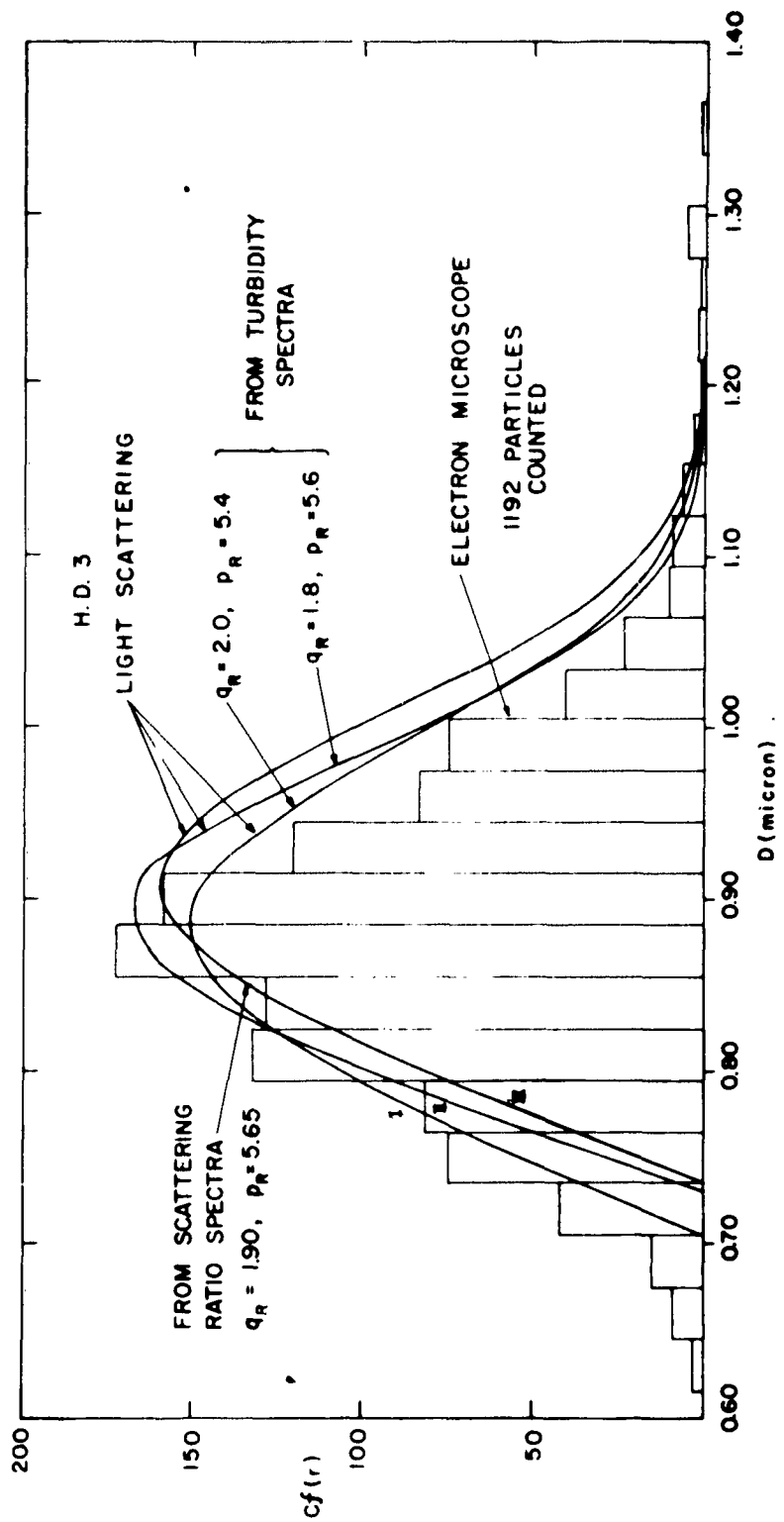
Contract Nonr 3511(00)   NR 051-380
                No. Copies   No. Copies

Commanding Officer
Office of Naval Research Branch Office
The John Crerar Library Building
86 East Randolph Street
Chicago 1, Illinois   (1)

Commanding Officer
Office of Naval Research Branch Office
346 Broadway
New York 13, New York   (1)

Commanding Officer
Office of Naval Research Branch Office
1030 East Green Street
Pasadena 1, California

Commanding Officer
Office of Naval Research Branch Office
Box 39 Navy No. 100 Fleet Post Office
New York, New York   (7)

Director, Naval Research Laboratory
Washington 25, D. C.
Attn: Technical Information Officer(6)
       Chemistry Division   (2)

Chief of Naval Research
Department of the Navy
Washington 25, D. C.
Attn: Code 425   (2)

DDR and E
Technical Library
Room 3C-128, The Pentagon
Washington 25, D. C.   (2)

Technical Director
Research and Engineering Division
Office of the Quartermaster General
Department of the Army
Washington 25, D. C.   (1)

Research Director
Clothing and Organic Materials Division
Quartermaster Research and Engineering Command
U. S. Army
Natick, Massachusetts

Air Force
Office of Scientific Research (SRC-E)
Washington 25, D. C.   (1)

Commanding Officer
Diamond Ordnance Fuze Laboratories
Washington 25, D. C.
Attn: Technical Information Office
       Branch 012   (1)

Office, Chief of Research and Development
Department of the Army
Washington 25, D. C.
Attn: Physical Sciences Division (1)

Chief, Bureau of Ships
Department of the Navy
Washington 25, D. C.
Attn: Code 342 C   (2)

Chief, Bureau of Naval Weapons
Department of the Navy
Washington 25, D. C.
Attn: Technical Library   (3)
       Code RRMA-3   (1)

ASTIA
Document Service Center
Arlington Hall Station
Arlington 12, Virginia   (10)

Director of Research
U. S. Army Signal Research and
   Development Laboratory
Fort Monmouth, New Jersey   (1)

Naval Radiological Defense Laboratory
San Francisco 24, California
Attn: Technical Library   (1)

Naval Ordnance Test Station
China Lake, California
Att: Head, Chemistry Division (1)
       Code 40   (1)
       Code 50   (1)

REVISED 1 FEB 1962

Contract Nonr 3511(00)   Wayne State University   NR No. 051-380

	No. Copies		No. Copies
Commanding Officer Army Research Office Box CM, Duke Station Durham, North Carolina Attn: Scientific Synthesis Office	(1)	Aeronautical Systems Division ASRCNP Wright-Patterson Air Force Base Ohio	(1)
Brookhaven National Laboratory Chemistry Department Upton, New York	(1)	Office of Chief of Engineers Research and Development Division Department of the Army Gravelly Point Washington 25, D. C.	(1)
Atomic Energy Commission Division of Research Chemistry Programs Washington 25, D. C.	(1)	Engineer Research and Development Laboratory Fort Belvoir, Virginia Attn: Materials Branch, Mr. Mitton	(1)
Atomic Energy Commission Division of Technical Information Extension Post Office Box 62 Oak Ridge, Tennessee	(1)	Commander Mare Island Naval Shipyard Rubber Laboratory Vallejo, California	(1)
U. S. Army Chemical Research and Development Laboratories Technical Library Army Chemical Center, Maryland	(1)	Dr. J. H. Faull, Jr. 72 Fresh Pond Lane Cambridge 38, Massachusetts	(1)
Office of Technical Services Department of Commerce Washington 25, D. C.	(1)	Dr. R. S. Stein Department of Chemistry University of Massachusetts Amherst, Massachusetts	(1)
Dr. Albert Lightbody Naval Ordnance Laboratory White Oak, Silver Spring, Md.	(1)	Dr. L. F. Rahm Plastics Laboratory Princeton University Princeton, New Jersey	(1)
Dr. W. H. Avery Applied Physics Laboratory The John Hopkins University 8621 Georgia Avenue Silver Spring, Md.	(1)	Dr. A. V. Tobolsky Department of Chemistry Princeton University Princeton, New Jersey	(1)
National Bureau of Standards Washington 25, D. C. Attn: Chief, Organic and Fibrous Materials Division	(1)	Dr. U. P. Strauss Department of Chemistry Rutgers - The State University New Brunswick, New Jersey	(1)
Chief, Bureau of Yards and Docks Department of the Navy Washington 25, D. C. Attn: Code P300	(1)		